Volume 16
Number 3
21 January 2025
Pages 983–1470

Chemical Science

rsc.li/chemical-science

ISSN 2041-6539

ROYAL SOCIETY OF CHEMISTRY

EDGE ARTICLE

Himanshu Mishra *et al.*

Why do some metal ions spontaneously form nanoparticles in water microdroplets? Disentangling the contributions of the air–water interface and bulk redox chemistry

15 YEARS ANNIVERSARY

Chemical Science

ROYAL SOCIETY OF CHEMISTRY

EDGE ARTICLE

View Article Online
View Journal | View Issue

Check for updates

Cite this: *Chem. Sci.*, 2025, **16**, 1115

All publication charges for this article have been paid for by the Royal Society of Chemistry

Open Access Article. Published on 18 November 2024. Downloaded on 2/16/2026 4:10:19 PM. This article is licensed under a Creative Commons Attribution-NonCommercial 3.0 Unported Licence.

Why do some metal ions spontaneously form nanoparticles in water microdroplets? Disentangling the contributions of the air–water interface and bulk redox chemistry†

Muzzamil Ahmad Eatoo,[abcd] Nimer Wehbe,[e] Najeh Kharbatia,[b] Xianrong Guo[e] and Himanshu Mishra *[abcd]

Received 16th May 2024
Accepted 13th November 2024

DOI: 10.1039/d4sc03217a

rsc.li/chemical-science

Water microdroplets containing 100 μM $HAuCl_4$ have been shown to reduce gold ions into gold nanoparticles spontaneously. It has been suggested that this chemical transformation takes place exclusively at the air–water interface of microdroplets, albeit without mechanistic insights. We compared the fate of several metallic salts in water, methanol, ethanol, and acetonitrile in the bulk phase and microdroplet geometry (sprays). Experiments revealed that when $HAuCl_4$ (or $PtCl_4$) is added to bulk water (or methanol or ethanol), metal NPs appear spontaneously. Over time, the nanoparticles grow, evidenced by the bulk solutions' changing colors. If the bulk solution is sprayed pneumatically and microdroplets are collected, the NP size distribution is not significantly enhanced. We find that the reduction of metal ions is accompanied by the oxidation of water (or alcohols); however, these redox reactions are minimal in acetonitrile. This establishes that the spontaneous reduction of metal ions is (i) a bulk phase phenomenon in water and several non-aqueous solutions, (ii) minimally affected by the air–water interface or the microdroplet geometry, and (iii) is not limited to Au^{3+} ions and can be explained *via* the electrochemical series. These results advance our understanding of aquatic chemistry and liquids in general and should be relevant in soil chemistry, biogeochemistry, electrochemistry, and green chemistry.

Introduction

Biochemistry, chemistry, and chemical engineering textbooks often limit the role of water in chemical reactions to dissolving/hydrating molecules and ions;[1–3] however, this view is rapidly evolving.[4–9] In the last two decades, experimental and computational studies have revealed that the skin of water – the air–water interface – and water–hydrophobe interfaces, in general, have anomalous features such as enhanced speciation of ions[10,11] and electrified interfaces.[12–15] Several studies have reported on orders of magnitude faster (*e.g.*, 10^2–$10^6\times$) reaction rates in water microdroplets compared with the bulk phase, thereby expanding the function of aqueous interfaces in chemical transformations beyond heat and mass transfer.[5,16–24] This exciting field – microdroplet chemistry – has emerged as a frontier in chemical science with potential implications for atmospheric aerosols,[25] sea sprays,[26] disease transmission,[27,28] life's origins,[16,19,29] the chemistry of clouds, fog, smog, and dew,[30–32] soil processes,[33] green chemistry,[18] hospital disinfection,[34] the food industry,[35] and fizzy beverages;[36] also, one may expect similar trends in microbubbles/foam in fermenter broths,[37] wastewater treatment,[38,39] and electrochemistry.[40,41]

While much excitement exists, several claims for purely interfacial effects being responsible for the rate enhancement have been challenged. This is because the vast majority of reports exploit electrospray ionization mass spectrometry (ESI-MS), which entails rapid solvent evaporation, solute concentration, temperature, electric field gradients, *etc.*, conditions that are far from thermodynamic equilibrium and, therefore, not representative of common systems.[20,23,42,43] For instance, the emergence of superacid chemistry in the microdroplets of mildly acidic water (pH < 4)[44,45] and the formation of abiotic sugar phosphates in water microdroplets[16] have been

[a]*Environmental Science and Engineering (EnSE) Program, Biological and Environmental Science and Engineering (BESE) Division, King Abdullah University of Science and Technology (KAUST), Thuwal, 23955-6900, Kingdom of Saudi Arabia. E-mail: himanshu.mishra@kaust.edu.sa*

[b]*Water Desalination and Reuse Center (WDRC), King Abdullah University of Science and Technology (KAUST), Thuwal, 23955-6900, Kingdom of Saudi Arabia*

[c]*Center for Desert Agriculture (CDA), King Abdullah University of Science and Technology (KAUST), Thuwal, 23955-6900, Saudi Arabia*

[d]*Interfacial Lab (iLab), King Abdullah University of Science and Technology (KAUST), Thuwal, 23955-6900, Saudi Arabia*

[e]*Core Labs, King Abdullah University of Science and Technology (KAUST), Thuwal, 23955-6900, Saudi Arabia*

† Electronic supplementary information (ESI) available. See DOI: https://doi.org/10.1039/d4sc03217a

© 2025 The Author(s). Published by the Royal Society of Chemistry

Open Access Article. Published on 18 November 2024. Downloaded on 2/16/2026 4:10:19 PM. This article is licensed under a Creative Commons Attribution-NonCommercial 3.0 Unported Licence.

challenged recently[46–49] (for recent reviews on this subject, see ref. 15, 24, 50 and 51). Controversial reports on microdroplet chemistry are not limited to ESIMS alone. For instance, recently, Zare & co-workers claimed that the air–water interface of microdroplets spontaneously generates H_2O_2,[52–55] and the reported amounts varied from ~1 ppm or 30 μM (in 2019 for pneumatically sprayed droplets)[52] to 114 μM (in 2020 for condensed droplets)[54] to 180 μM (in 2021 for microdroplets condensed at 55% or 70% relative humidity).[53] As for the mechanistic insights, computer simulations of Head-Gordon & co-workers[56–58] have suggested the emergence of instantaneous ultrahigh electric fields at the air–water interface that may drive H_2O_2 formation, while the simulations of Ruiz-López and co-workers[50] and Gong and co-workers[59] suggested that the local electric field was lower at the air–water interface compared to the bulk. Cooks and co-workers have speculated that the air–water interface of microdroplets promotes the formation of water radical cations H_2O^+* and anions H_2O^-*, which constitute the primary redox species.[24] Colussi[60] also proposed a similar mechanism whereby spraying yielded a small fraction of oppositely charged droplets, *i.e.*, comprising excess H_3O^+ and OH^-, and these droplets collided to form OH* and H* radicals.[60] Our team has challenged these reports[24,27,52–57,60] by pinpointing the artifacts arising due to the ambient ozone contamination,[61] and OH* radical formation due to ultrasonication;[62] also, we have explained the appearance of trace (~1 μM) H_2O_2 concentrations in pneumatic sprays based on the reduction of dissolved oxygen gas at water–solid interfaces.[63]

In a recent feature by the Royal Society of Chemistry's magazine, *Chemistry World*, entitled, "Why is Microdroplet Chemistry Contentious?",[64] the following excerpt appeared, "*Zare's team made its hydrogen peroxide discovery while trying to synthesize gold nanostructures in microdroplet, armed with the knowledge that Michael Faraday had made gold films with lemon juice. They added sodium borohydride – which Zare calls modern lemon juice – to water microdroplets and found that the reaction occurred 100 000 times faster than in bulk liquid. As a control experiment, the team removed the reducing agent – the sodium borohydride – yet still produced gold nanoparticles. That was a shock to us, says Zare*." In response, here, we extend our investigation of H_2O_2 production in water microdroplets to the spontaneous reduction of Au^{3+}(aq) to Au nanoparticles (Au NPs) containing chloroauric acid ($HAuCl_4$, 100 μM concentration).[65] Zare and colleagues have speculated that this chemical transformation occurs exclusively at the air–water interface. While it has been reported that gold nanoparticles can be formed in bulk water by supplying energy *via* microwaves,[66] how water microdroplets (*i.e.*, the air–water interface) drive this transformation without an external energy source, *e.g.*, electrical voltage or reducing agent, has baffled chemists. Here, we resolve this mystery by addressing the following questions:

(1) Is the spontaneous reduction of gold in water limited only to water microdroplets, or does it also occur in bulk water?

(2) If gold ions get spontaneously reduced inside water, does water get oxidized? Is there a peroxide connection?

(3) What are the effects of the concentration of Au^{3+} ions, the water pH, and dissolved oxygen gas on the NP formation?

(4) Do other metallic ions, *e.g.*, Pt^{4+}, Al^{3+}, Fe^{3+}, Gd^{3+}, Fe^{2+}, Cu^{2+}, Mg^{2+}, Ni^{2+}, Zn^{2+}, and Na^+, also exhibit this behavior?

(5) Does the air–water interface have unique features to form Au NPs, or can other common liquids such as ethanol, methanol, and acetonitrile also drive the spontaneous reduction of metallic ions?

Our experiments reveal that when salts containing Au^{3+} (or Pt^{4+} or Fe^{3+}) ions are added to water they undergo spontaneous reduction in the bulk phase as well as in microdroplets. In fact, in this study, whenever NPs formed for a specific salt–solvent system, they formed both in the bulk phase and in the sprayed microdroplets. There was no scenario wherein the spontaneous reduction of Au^{3+} ions occurred exclusively inside microdroplets but not in bulk.

Results

In this work, we used MilliQ Advantage 10 (18 MΩ cm) deionized water, albeit the results were identical with HPLC grade water. Microdroplets were generated *via* pneumatic nebulization following the protocols of Zare *et al.*[65] Briefly, the spray device comprised two concentric capillaries, and the solution was injected through a 0.1 mm-wide inner stainless-steel capillary at a rate of 25 μL min^{-1}. The solution was sheared *via* high-pressure dry N_2 gas flowing through the outer concentric capillary at 100 psi, forming a microdroplet stream (ESI Fig. S1†).

The effects of the air–water interface on NP formation were analyzed by spraying 100 μM aqueous $HAuCl_4$ solution *via* pneumatic nebulization, which yielded microdroplets of an average size of ~20 μm (ESI Fig. S1†). In a typical experiment, microdroplets were formed and collected in clean glass vials; also, the effects of solvent evaporation during spraying were compensated by adding bulk water to the glass vials to restore the original (bulk) salt concentration. Then microdroplets of the solution were transferred onto transmission electron microscopy (TEM) grids and SiO_2/Si wafers for TEM and scanning electron microscopy (SEM), respectively. Both techniques revealed NP formation in sprays. Curiously, the transparent mother solution (100 μM aqueous $HAuCl_4$ stored at 22 °C inside a laboratory) changed its color to red in 2–3 days and blue in 2–3 weeks (Fig. 2a). The TEM analysis of samples drawn from the mother solutions revealed the presence of gold NPs (Fig. 2c and d, and S3†). Dynamic light scattering (DLS) showed the appearance of a bimodal nanoparticle size distribution in the freshly prepared solutions composed of NPs and aggregates (Fig. 2b and S11b†). X-ray photoelectron spectroscopy (XPS) compared the oxidation states of gold in the newly prepared and one-week-old solutions (Fig. 2e and S11(e),† Methods). The oxidation state of gold in the freshly prepared solutions was +3 and +1, which indicated that the reduction was spontaneous, whereas the dominant oxidation state of gold in the 1 week-old samples was 0. These results demonstrate that the reduction of gold ions occurs spontaneously in bulk water and is not exclusive to the microdroplet environment/geometry.

Next, we investigated whether the microdroplet environment, *i.e.*, the air–water interface, considerably accelerated the

© 2025 The Author(s). Published by the Royal Society of Chemistry

Open Access Article. Published on 18 November 2024. Downloaded on 2/16/2026 4:10:19 PM. This article is licensed under a Creative Commons Attribution-NonCommercial 3.0 Unported Licence.

rate of reduction and nanoparticle formation compared with the bulk phase. To this end, bulk solutions of the same concentration (100 μM $HAuCl_4$) but different ages, *i.e.*, varying from seconds to minutes to hours, were pneumatically sheared into water microdroplets (Fig. 1). The flying microdroplets were then intercepted and collected (in the liquid state, *i.e.*, before complete evaporation) and analyzed *via* DLS. The observed particle size distributions were compared against those of the mother solution (Fig. S4†). Results revealed that the microdroplets afforded no significant enhancement in the particle sizes over the bulk phase, demonstrating that microdroplets do not have any significant effect on the formation or growth of nanoparticles. In summary, the reduction of gold ions in bulk water is spontaneous, and microdroplets are not essential, or the size of microdroplets is not the driving force for the spontaneity of this reduction reaction.

Since the formation of AuNPs from Au^{3+} is a reduction reaction, a parallel oxidation reaction must occur simultaneously. Therefore, to reveal the redox reaction's oxidation half-reaction, we performed solution-state NMR spectroscopy to investigate the possible oxidation products in a liquid state. Gas chromatography (GC) was performed to determine the evolution of the formed gases. NMR spectroscopy revealed the spontaneous formation of H_2O_2(aq) in the bulk $HAuCl_4$ solution, and GC revealed the gradual evolution of oxygen (O_2) gas in the headspace (Fig. 3a and S5†). The formation of H_2O_2 was also quantified using a Hydrogen Peroxide Assay Kit (HPAK) (Fig. 3b). The mechanistic insights into this chemistry are presented in the Discussion section.

Fig. 3a presents H-NMR data comparing H_2O_2 formation in freshly prepared 0.3 M $HAuCl_4$ solution in MilliQ water against a freshly prepared 0.3 M $HAuCl_4$ solution in 200 μM standard H_2O_2 solution. The presence of only one peak in both the solutions, at 9.4 ppm, is observed by following the protocol of Bax and co-workers (detection limit ≥50 nM).[67] Using the same technique, we found that the concentration of $HAuCl_4$ increases in the aqueous solution, so does the spontaneous H_2O_2(aq) formation (Fig. 3b), *i.e.*, they appear to be stoichiometric (see Discussion). We also examined H_2O_2(aq) formation in $HAuCl_4$ solutions prepared using water with dissolved oxygen and deoxygenated water. The dissolved oxygen had no measurable effect on H_2O_2 formation in these experiments (Fig. S6†). Thus, we confirmed that the formation of H_2O_2(aq) in bulk water is the oxidation half-reaction during the spontaneous formation of Au NPs.

Next, we investigated the effects of the solution pH and concentration of Au^{3+} ions on the formation of AuNPs and corresponding H_2O_2 produced. As the solution turned acidic, the formation of the AuNPs and H_2O_2 decreased (Fig. 4a–d). SEM imaging revealed that when a 200 μM $HAuCl_4$ solution was prepared using deionized water, or 0.1 M HCl, or 1 M HCl, the nanoparticles were well-formed (Fig. 4b), or smaller and fewer (Fig. 4c), or nearly absent (Fig. 4d), respectively. This indicates that gold ions are more stable in lower pH or highly acidic aqueous solutions. Following this observation, we investigated the effects of the gold ion concentration on the formation of Au NPs and H_2O_2. Experimental results revealed that gold ions could undergo complete reduction to form Au NPs in relatively diluted solutions (<0.05 M), whereas in concentrated solutions (>0.05 M), Au^{3+} primarily reduced to lower oxidation states (mostly Au^{+1}), while H_2O_2 was produced stoichiometrically. XPS pinpointed that as the salt concentration increased, the ratio of hydrated ions Au^{1+}/Au^{3+} decreased (Fig. 4e).

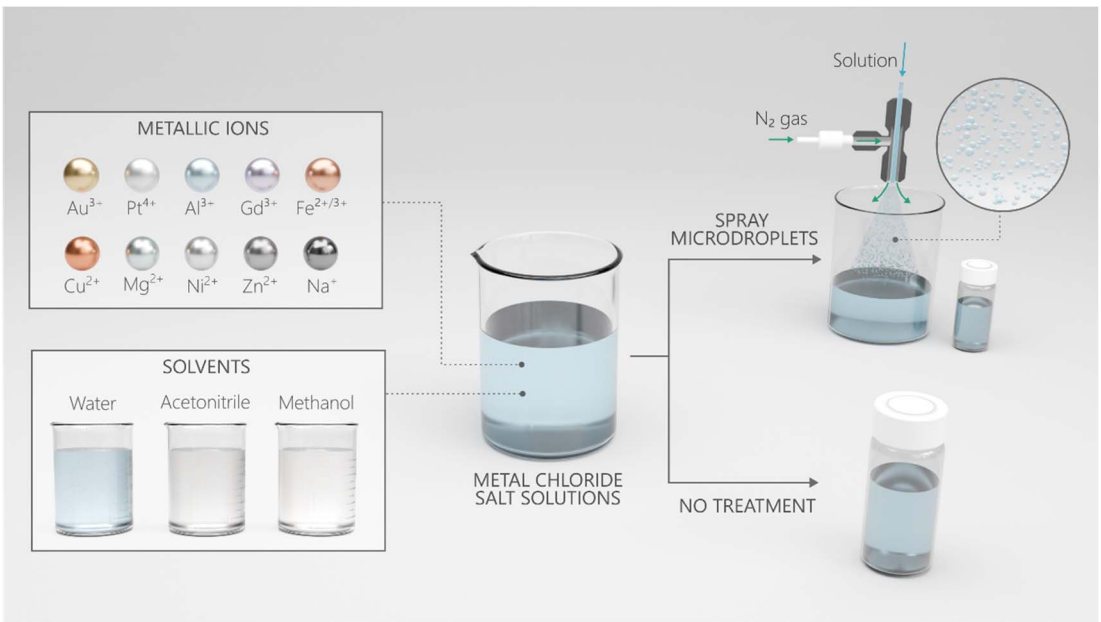

Fig. 1 Experimental design composed of solutions made from a variety of metallic salts and solvents. Nanoparticle formation was probed in bulk solutions and sprayed microdroplets to disentangle the contributions of bulk redox chemistry, microdroplet geometry, and the air–water interface.

Open Access Article. Published on 18 November 2024. Downloaded on 2/16/2026 4:10:19 PM. This article is licensed under a Creative Commons Attribution-NonCommercial 3.0 Unported Licence.

To further elucidate whether the mechanism underlying this chemical transformation, *i.e.*, the spontaneous reduction of Au^{3+} in water, is unique or in common with other metal ions, aqueous solutions of a few common metal ions such as Pt^{4+}, Al^{3+}, Fe^{3+}, Gd^{3+}, Fe^{2+}, Cu^{2+}, Mg^{2+}, Ni^{2+}, Zn^{2+}, and Na^{+} were studied. We found that two metal cations, Pt^{4+} and Fe^{3+}, also produced H_2O_2 in water (Fig. 5c and d), while the remaining metallic ions did not produce H_2O_2 in bulk solutions (or microdroplets). Notably, considerably higher amounts of H_2O_2 were produced by Au^{3+} reduction than those produced *via* Pt^{4+} and Fe^{3+} reduction.

XPS analysis confirmed that Pt^{4+} and Fe^{3+} were spontaneously reduced in water similar to Au^{3+}, yielding Pt^{2+} and Fe^{2+} (Fig. 5a and b), and the formation of Pt NPs was observed by TEM imaging (Fig. S7†). Notably, the reduction of Fe^{3+} to its zero-valent form was not observed. In other words, of all the metal ions studied herein, the pure metallic form of NPs was only observed in $HAuCl_4$ and $PtCl_4$ solutions.

Discussion

This section consolidates all the findings and presents mechanistic insights. Our experiments have revealed that Au^{3+} ions from $HAuCl_4$ get spontaneously reduced in bulk water, forming Au NPs and generating H_2O_2(aq). Spraying bulk solutions (freshly prepared or aged) and collecting the microdroplets reveal no significant enhancement in the size of AuNPs, suggesting that the microdroplet environment's effects, if any, are minor, such as facilitating solvent evaporation. Based on our experimental results, wherein Au^{3+} ions in bulk $HAuCl_4$ solutions spontaneously reduce to Au^{+} ions and AuNPs and drive the formation of H_2O_2(aq) (Fig. 2, 3, and S5†) and decrease in the solution pH, we suggest the following half-reactions:[40,68]

Reduction half-reactions:

$$AuCl_4^-(aq) + 3e^- \rightleftharpoons Au(s) + 4Cl^-,\ E^\circ\ (\text{volts}): 1.002 \quad (1)$$

$$AuCl_4^-(aq) + 2e^- \rightleftharpoons AuCl_2^-(aq) + 2Cl^-,\ E^\circ\ (\text{volts}): 0.92 \quad (2)$$

Possible feasible oxidation half-reactions that may drive the above reduction reactions:

$$O_2(aq) + 2H_2O(aq) + 4e^- \rightleftharpoons 4OH^-(aq),\ E^\circ\ (\text{volts}): 0.40 \quad (3)$$

$$H_2O_2 + H^+ + e^- \rightleftharpoons HO^* + H_2O,\ E^\circ\ (\text{volts}): 0.39 \quad (4)$$

$$O_2(aq) + 2H^+ + 2e^- \rightleftharpoons H_2O_2,\ E^\circ\ (\text{volts}): 0.69 \quad (5)$$

The standard reduction potentials of eqn (1) and (2) are higher than those of eqn (3) and (4); therefore, it is possible that OH^-(aq) ions (eqn (3)) and H_2O may be oxidized to form H_2O_2(aq) (eqn (4)), which later decomposes/oxidizes gradually with time and forms O_2(g) (eqn (5)) further reducing gold ions.

Out of curiosity, we also probed the behavior of $HAuCl_4$ in methanol, ethanol, and acetonitrile, to see if there was something special about water in the nanoparticle formation. We observed that Au^{3+} reduced faster in methanol (and ethanol)

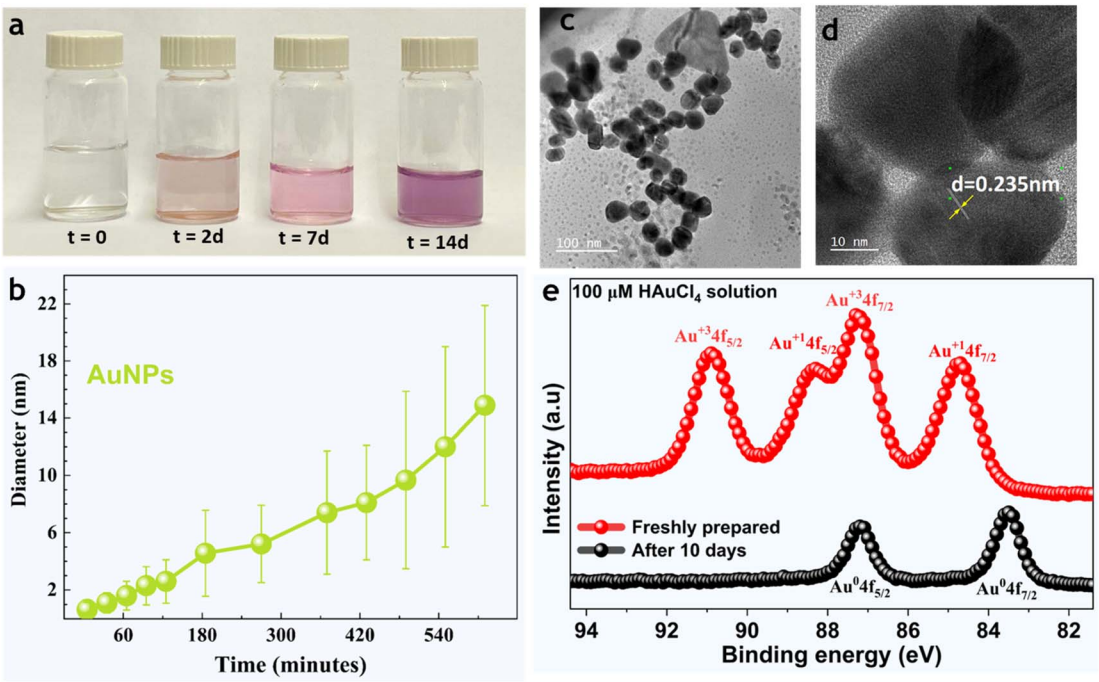

Fig. 2 Spontaneous formation and growth of AuNPs in bulk 100 μM $HAuCl_4$ in water. (a) Bulk solution changing color due to the nucleation and growth of AuNPs. (b) Formation and growth of particles with time, as measured by DLS. (c) TEM micrograph showing the presence of AuNPs of different sizes. (d) TEM imaging showing an interlayer spacing of ~0.235 nm corresponding to the Au(111) atomic plane of metallic gold Au(0). (e) XPS analysis showing the presence of Au^{3+} and Au^{+} in the freshly prepared solution and Au(0) in the 10-days-old solution, revealing the complete reduction of gold ions to AuNPs after some time.

© 2025 The Author(s). Published by the Royal Society of Chemistry

Open Access Article. Published on 18 November 2024. Downloaded on 2/16/2026 4:10:19 PM.
This article is licensed under a Creative Commons Attribution-NonCommercial 3.0 Unported Licence.

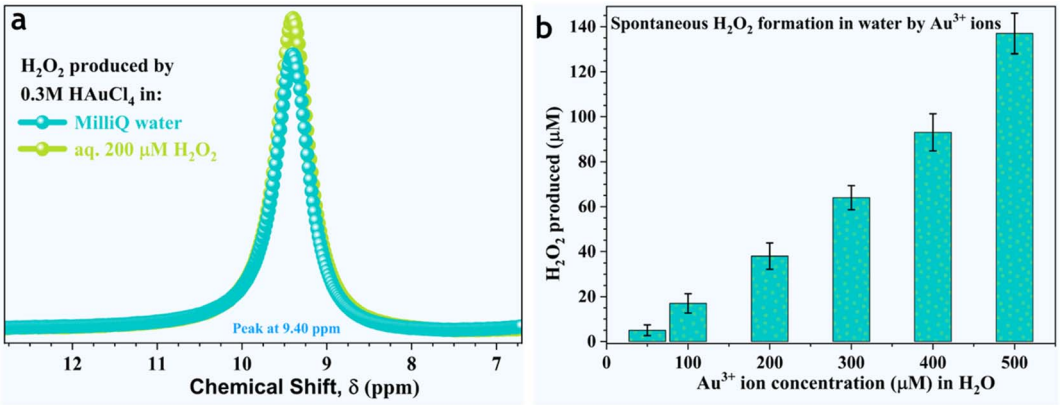

Fig. 3 Production of H_2O_2 during the reduction of Au^{3+} ions in bulk water. (a) NMR spectroscopy pinpoints the formation of H_2O_2. (b) Quantification of H_2O_2 in freshly prepared aqueous solutions as a function of $HAuCl_4$ concentration.

than in bulk water, and it was negligible/sluggish in acetonitrile (Fig. 6a and b). The formation of Au NPs in methanol was accompanied by the formation of H_2O_2 (Fig. S12†), methylal ($CH_3OCH_2OCH_3$), and dimethyl ether (CH_3OCH_3) (Fig. S8†). Note: our investigation of the spontaneous formation of gold nanoparticles in the organic solvents was merely a curiosity, and an in-depth investigation of reaction byproducts and underlying mechanisms falls out of the scope of this manuscript. Lastly, in a complementary experiment, we quantified the amount of the reducing agent (standard hydrogen peroxide, 30%) required to completely reduce a fixed concentration of gold solution (0.1 M $HAuCl_4$) in methanol, water, and acetonitrile. The volume percent of H_2O_2 required was 0.4 ± 0.1, 1.0 ± 0.2, and 35 ± 1, respectively.

Now we discuss why some of the metal ions formed NPs in water, while others did not. For instance, we found that Pt^{4+}(aq) was reduced to Pt(s) NPs and Pt^{2+}(aq), whereas Fe^{3+}(aq) was reduced only to Fe^{2+}(aq) ions and Fe^0(s) was not observed (Fig. 5 and S7†). Our observation about Fe is substantiated by the NIST XPS database[69] and high-resolution XPS spectra (Fig. 5b) in which the Fe 2p peak is broad and asymmetric, suggesting at least two oxidation states of Fe in the solution (Fig. 5b). The bottom line is that the reduction potentials of Pt^{4+}(aq) to Pt(s) and Pt^{2+}(aq) and that of Fe^{3+}(aq) to Fe^{2+}(aq) were more thermodynamically favored than the water oxidation reactions ((eqn (3) & (4) and ESI Table S2†). As the reduction potentials of Fe^{3+}(aq) and Fe^{2+}(aq) to Fe(s), *i.e.*, −0.037 and −0.44 V, are lower than those listed in eqn (3) and (4), it is not feasible for Fe^{3+}(aq) or Fe^{2+}(aq) to reduce to Fe(s) by water. Similarly, the spontaneous reduction of Al^{3+}, Cu^{2+}, Ni^{2+}, Zn^{2+}, and Mg^{2+} ions in water was also blocked (ESI Table S2†).

Next, we discuss the connection of the present findings with our recent reports unraveling the factors and mechanisms underlying the spontaneous formation of ~1 μM H_2O_2(aq) in

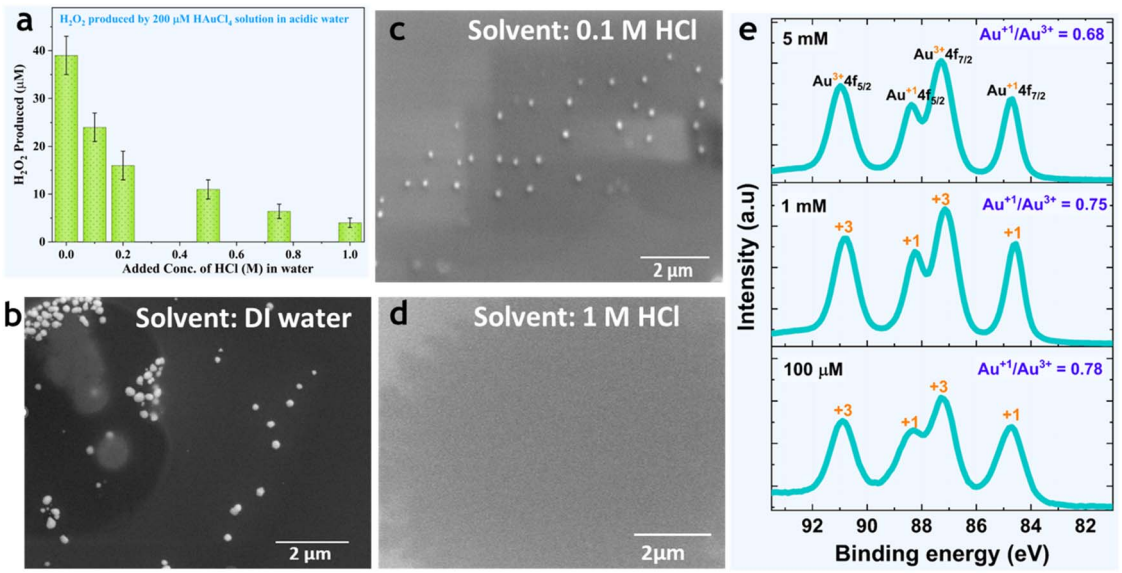

Fig. 4 Effects of the solution pH and concentration on the reduction of gold ions: (a) decrease in the rate of H_2O_2 production in bulk solutions as a function of HCl concentration (or pH) for a fixed $HAuCl_4$ concentration. Representative scanning electron micrographs (SEM) of gold NPs formed in a 200 μM $HAuCl_4$ solution formed with: (b) deionized water, (c) 0.1 M HCl, and (d) 1 M HCl solution. (e) XPS reveals the ratio of Au^{1+}/Au^{3+} in freshly prepared $HAuCl_4$ solutions of varying concentrations (100 μM, 1 mM, and 5 mM).

Open Access Article. Published on 18 November 2024. Downloaded on 2/16/2026 4:10:19 PM.
This article is licensed under a Creative Commons Attribution-NonCommercial 3.0 Unported Licence.

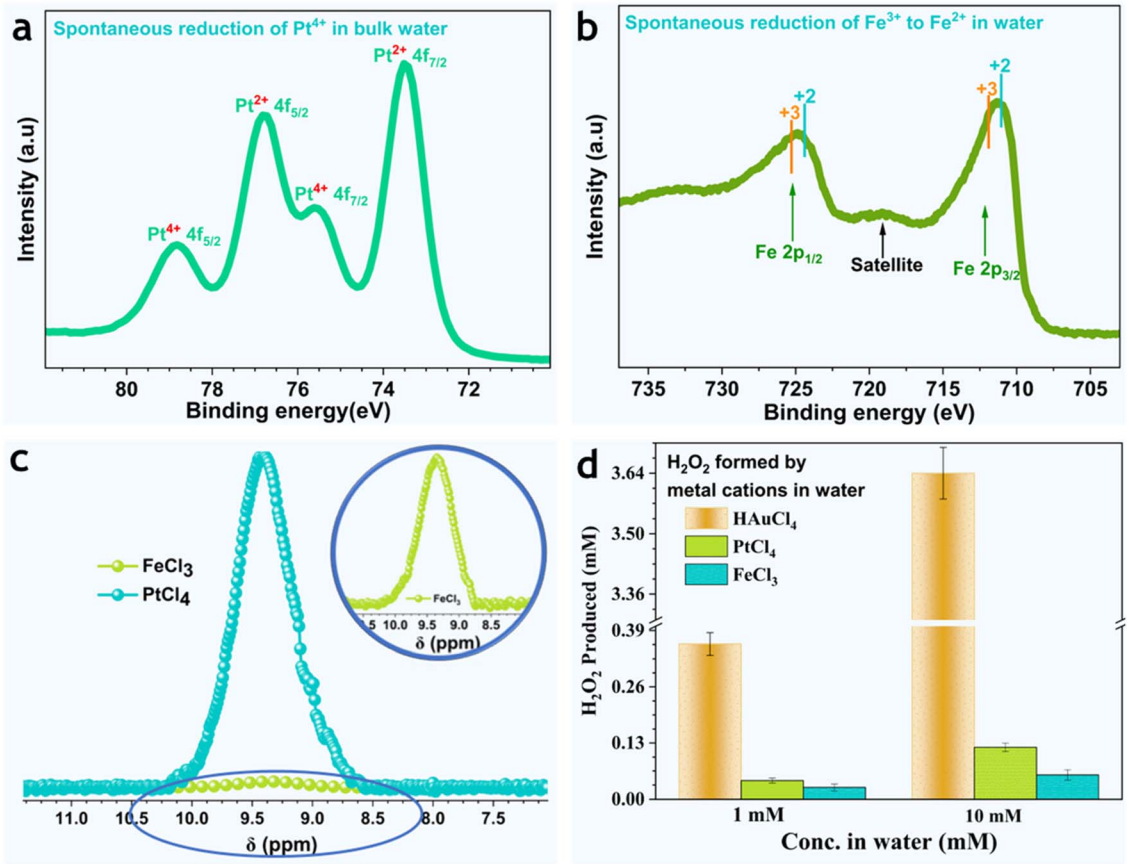

Fig. 5 Spontaneous reduction of metal ions, besides Au^{3+}, in water, which yields H_2O_2(aq). (a) XPS results of 100 μM $PtCl_4$ in water showing the reduction of Pt^{4+} to Pt^{2+}; Pt NPs observed *via* TEM images (Fig. S7†). (b) XPS results of $FeCl_3$ in water showing the spontaneous reduction of Fe^{3+} ions to Fe^{2+}. (c) NMR spectra confirming the formation of H_2O_2(aq) in aqueous solutions of $FeCl_3$ and $PtCl_4$ in water (each at a 100 μM initial concentration). (d) Comparison of H_2O_2(aq) formed by different concentrations of Au^{3+}, Pt^{4+}, and Fe^{3+} in water.

water microdroplets.[61–63] We have established that H_2O_2(aq) formation is independent of the air–water interface or the microdroplet geometry. Instead, it entails the reduction of dissolved O_2(aq) at the numerous water–solid interfaces involved in such experiments, such as pipes, tubing, containers, vials, plates, *etc.* Conversely, if dissolved O_2(aq) is removed from water, then H_2O_2(aq) formation is not observed in bulk, films, or microdroplets within a limit of detection of 50 nM. While some reports have corroborated our findings,[70–74] others have disagreed.[75–78] In contrast, the spontaneous NP formation and H_2O_2(aq) generation in water (bulk, films, or microdroplets) are driven by the reduction potential of metal ions and their concentration, and can be explained simply *via* the electrochemical series.[40]

Here we list some limitations of this study. First, we did not focus on the shape specificity of the nanoparticles/nanowires as a function of the bulk $HAuCl_4$ concentration or as a function of solvent evaporation during spraying. Experiments with bulk $HAuCl_4$ solutions revealed that as the salt concentration exceeded 200 μM, nanowires began to appear – in bulk and in sprayed microdroplets without detectable differences (Fig. S13†). We note that if the solvent evaporation during pneumatic spraying becomes excessive, a regime that we did not study, we anticipate the precipitation of $HAuCl_4$ salt out of water, *i.e.*, we do not expect a new interfacial chemistry to arise such that Au^{3+} ions specifically start reducing at the air–water interface to form Au NPs. Lastly, we did not take any special precautions to eliminate the existing nanoparticle impurities in the stock salts that may have accelerated the nucleation of nanoparticles in bulk solutions.[79]

In summary, our report refutes the claims that water microdroplets or the air–water interface has unique properties that can drive the spontaneous reduction of gold ions. This chemical reduction takes place in the bulk phase, and it is not limited to (i) gold ions, or (ii) water as a solvent, or (iii) microdroplets or the air–water interface. The entire phenomenon can be explained by the standard electrochemical series, *i.e.*, cations with very high reduction potential such as Au^{3+} and Pt^{4+} are so unstable that they can oxidize the solvent (water, methanol, and ethanol) to form NPs and H_2O_2(aq) and other byproducts in the case of alcohols. These findings advance our understanding of aquatic chemistry and warrant caution in investigating microdroplet chemistry and its environmental and practical relevance.

Methods

Chemicals

Gold(III) chloride trihydrate ($HAuCl_4 \cdot 3H_2O$, 520918), platinum(IV) chloride ($PtCl_4$, 206113), iron(III) chloride hexahydrate

© 2025 The Author(s). Published by the Royal Society of Chemistry

Open Access Article. Published on 18 November 2024. Downloaded on 2/16/2026 4:10:19 PM.
This article is licensed under a Creative Commons Attribution-NonCommercial 3.0 Unported Licence.

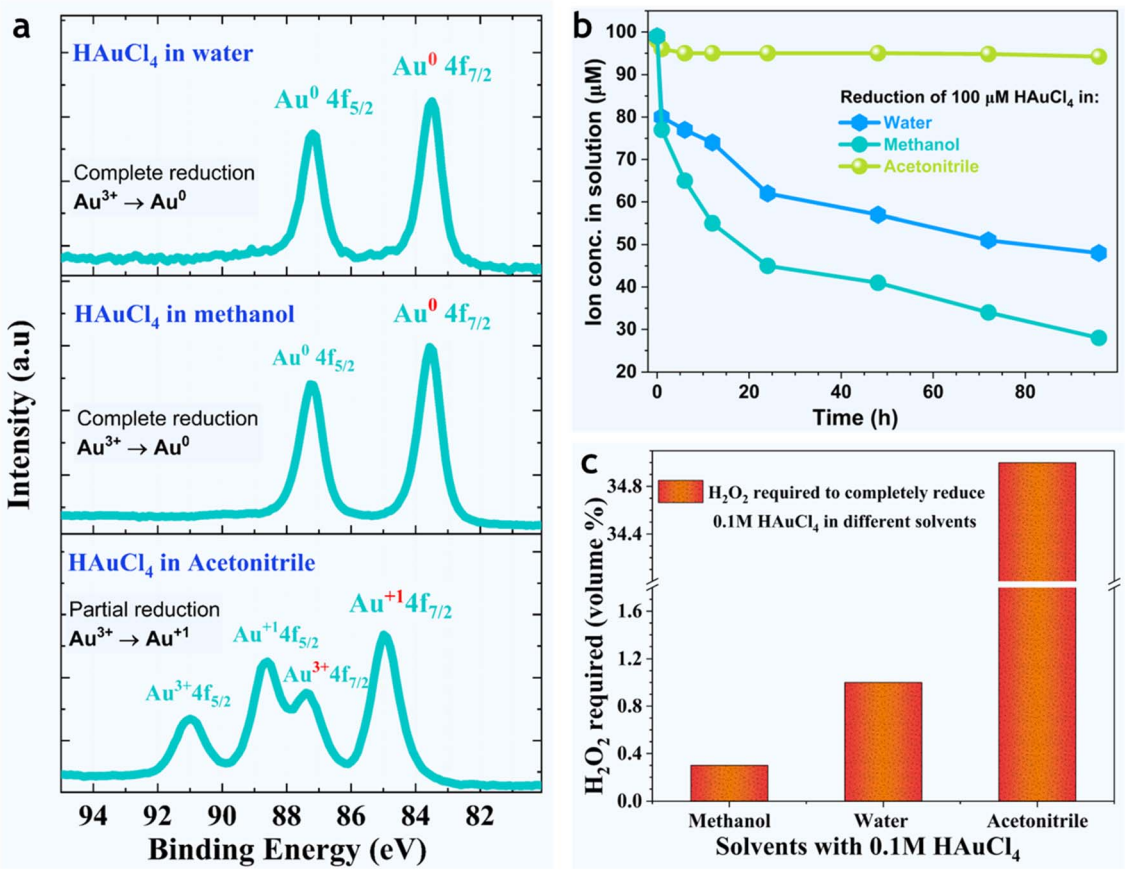

Fig. 6 Reduction of gold ions in different solvents. (a) Reduction of Au^{3+} in water, methanol, and acetonitrile. (b) Time-dependence of Au^{3+} ion concentration in water, methanol, and acetonitrile (all starting with 100 μM $HAuCl_4$) follows the trend: MeOH > H_2O ≫ CH_3-CN. (c) As a reducing agent, the amount of concentrated (30% v/v) H_2O_2 required for the complete reduction of 0.1 M $HAuCl_4$ in water, methanol, and acetonitrile. Since the amount of H_2O_2 required follows the trend: MeOH < H_2O ≪ CH_3-CN, it demonstrates that gold ions can undergo spontaneous (complete) reduction in water and methanol but not in acetonitrile. Note: the behaviors of methanol and ethanol were similar (Fig. S12†).

($FeCl_3 \cdot 6H_2O$, 10025-77-1), iron(II) chloride ($FeCl_2$, 37287-0), aluminum(III) chloride ($AlCl_3$, 06220), zinc chloride ($ZnCl_2$, 211273), magnesium chloride hexahydrate ($MgCl_2 \cdot 6H_2O$, 13152), sodium chloride (NaCl, 7647145), ammonium chloride (NH_4Cl, 213330), and copper chloride ($CuCl_2$, 7447394) were used. The following liquids were also used: deuterium oxide (D_2O, 3000007892), methanol-D4+0.03%TMS, acetonitrile-D3 (CAS 2206-26-0), acetonitrile (HPLC grade purchased from Fisher Scientific, batch 1072451), methanol (HPLC LC-MS grade), standard hydrogen peroxide (H_2O_2) 30% (Cat. 270733), HPLC grade water (Cat. 2594649), and deionized water (DI) obtained from a MilliQ Advantage 10 set-up (with resistivity 18.2 MΩ cm).

Characterization of NPs

SEM and TEM analyses were performed to characterize the NPs in the bulk solutions. For SEM, a small drop of liquid containing NPs was drop-coated on a silicon wafer substrate, and the solution was dried at room temperature. TEM images were acquired using a Titan ST Image Corrected (Thermo Fisher) instrument operated at a 300 kV acceleration voltage. EDS spectra and maps were acquired in the STEM mode using a four-quadrant SuperX EDS detector. For sample preparation, a drop of solution was placed on an ultra-thin carbon-coated holey copper grid, blotted with filter paper, and dried under ambient conditions. The presence and growth of NPs were examined *via* DLS. The growth of Au NPs was observed in 100 μM $HAuCl_4$ bulk solution at varying time scales.

XPS measurements

For the XPS studies of gold ion reduction in water, 100 μM $HAuCl_4$ solution was used. The drop coating method was employed to prepare the samples using silicon wafers, and Baer's method was closely followed.[80] A Kratos Axis Supra instrument equipped with a monochromatic Al Kα X-ray source ($h\nu$ = 1486.6 eV) operating at a power of 75 W and under UHV conditions in the range of $\sim 10^{-9}$ mbar was used to obtain the data. All the spectra were recorded in hybrid mode, using magnetic and electrostatic lenses and an aperture slot of 300 μm × 700 μm. The high-resolution spectra were acquired at

Open Access Article. Published on 18 November 2024. Downloaded on 2/16/2026 4:10:19 PM. This article is licensed under a Creative Commons Attribution-NonCommercial 3.0 Unported Licence.

a fixed analyzer pass energy of 20 eV. The samples were mounted in a floating mode to avoid differential charging.

Quantification of H_2O_2

H_2O_2 concentration in all the diluted salt solutions was quantified using a hydrogen peroxide assay kit (HPAK). This is based on the principle that when hydrogen peroxide maintains contact with the AbIR peroxidase indicator, it causes fluorescence. Its maximum emission and excitation wavelengths are 674 and 647 nm, respectively. The samples were analyzed by mixing 50 μL of HPAK reaction mixture with 50 μL of samples in a 96-well black/transparent bottom microtiter plate using a SpectraMax M3 microplate reader. For the fluorescence reading, the SoftMax Pro 7 software was used. H_2O_2 in the samples was quantified using the calibration curve obtained from the standard samples on the same day.

Peroxide test strips for semi-quantitative analysis. For the qualitative estimation of H_2O_2 in the aqueous samples, peroxide test strips (Baker Test Strips purchased from VWR International) with a detection limit of 1 ppm were used. These strips use a colorimetric reagent that changes to blue when in contact with H_2O_2.

NMR spectroscopy for H_2O_2(aq) quantification

NMR measurements were performed on a 700 MHz Bruker Avance Neo NMR spectrometer equipped with a 5 mm *Z*-axis gradient TXO Cryoprobe at 275 K. For water samples, a 6 ms Gaussian 90-degree pulse was applied to excite the proton of hydrogen peroxide, followed by a 50 ms acquisition and a 1 ms recycle delay. For acetonitrile samples, a W5 binomial pulse sequence with gradients or a routine 1D proton pulse was applied for solvent suppression or non-suppression measurements, respectively. Peak quantification and peak position confirmation of H_2O_2 in salt solutions were performed by comparing the results obtained for standard H_2O_2 samples.

GC-MS experiment

The methanol sample was extracted by adding 2 mL each of water and hexane to initiate phase separation. Approximately 1 μL of the top hexane layer was analyzed using a single quadrupole GC-MS system (Agilent 7890 GC/5975C MSD) coupled to an EI source with an ionization energy of 70 eV. The ion source and mass analyzer temperatures were kept at 230 °C and 150 °C, respectively, with a solvent delay of 0 min. The mass analyzer was tuned according to the manufacturer's instructions, and the scan was fixed at 15–200 Da. A DB-5MS fused silica capillary column (30 m × 0.25 mm I.D., 0.25 μm film thickness; Agilent J&W Scientific, Folsom, CA) was used for chromatographic separation; the column contained a 5% phenyl and 95% methylpolysiloxane cross-linked stationary phase. Furthermore, helium was the carrier gas at a constant flow rate of 1.0 mL min^{-1}. The sample was injected into a 6890A gas chromatograph (Agilent, USA). The oven program was set to 30 °C and held for 10 min; the temperature was ramped at 20 °C min^{-1} to 260 °C with a 0 min hold time. The GC inlet temperature was set at 250 °C, and the transfer line temperature to the MS EI source was kept at 320 °C. The sample was injected using an autosampler equipped with a 10 μL syringe into a split/splitless inlet with a split ratio 10 : 1.

Oxygen gas analysis

Headspace analysis of the aqueous $HAuCl_4$ solution was performed using a gas analyzer (Model 310C, SRI, USA) equipped with a thermal conductivity detector (TCD). About 1 mL of the headspace above the sample was withdrawn using a gas-tight syringe (Hamilton, USA) and injected into a 6-foot molecular sieve 13× packed column. The oven temperature of the column was set to 100 °C with argon as the carrier gas.

Data availability

All data needed to evaluate the conclusions in the paper are present in the paper or the ESI.†

Author contributions

ME and HM designed the experiments, which ME performed. NK and ME performed LC-MS, GC, and ICP-OES experiments. XG and ME performed NMR spectroscopy experiments. NW and ME performed XPS studies. HM and ME wrote the manuscript.

Conflicts of interest

The authors declare no competing interests.

Acknowledgements

HM acknowledges KAUST for funding (Grant No. BAS/1/1070-01-01). The co-authors thank Dr Adair Gallo, Dr Peng Zhang, and Ms Nayara Musskopf for building a robust experimental setup in HM's laboratory; Dr Ryo Mizuta, Scientific Illustrator at KAUST, for preparing illustrations in Fig. 1; Dr Valentina-Elena Musteata, scientist from IAC at KAUST for her assistance with TEM; Mohammed Abdulwahab ElShaer from WDRC at KAUST for his assistance with DLS and Usman Sharif from Laboratory Equipment Maintenance (LEM) team at KAUST for his contribution to maintaining the XPS instrument at the best operating conditions.

References

1 R. H. Bruce Alberts, A. Johnson, D. Morgan, M. Raff , K. Roberts, *Peter Walter Molecular Biology of the Cell*, W. W. Norton & Company, 7th edn, 2022.
2 J. K. Rob Phillips, J. Theriot, H. Garcia, *Physical Biology of the Cell Garland Science*, 2012.
3 R. J. Davis and M. E. Davis, *Fundamentals of Chemical Reaction Engineering*, Dover Publications, 2013.
4 W. Bal, E. Kurowska and W. Maret, The Final Frontier of pH and the Undiscovered Country Beyond, *PLoS One*, 2012, **7**, e45832.

© 2025 The Author(s). Published by the Royal Society of Chemistry

Open Access Article. Published on 18 November 2024. Downloaded on 2/16/2026 4:10:19 PM. This article is licensed under a Creative Commons Attribution-NonCommercial 3.0 Unported Licence.

5 M. F. Ruiz-Lopez, J. S. Francisco, M. T. C. Martins-Costa and J. M. Anglada, Molecular reactions at aqueous interfaces, *Nat. Rev. Chem*, 2020, **4**, 459–475.
6 E. M. Stuve, Ionization of water in interfacial electric fields: An electrochemical view, *Chem. Phys. Lett.*, 2012, **519–520**, 1–17.
7 P. Ball, Water as an Active Constituent in Cell Biology, *Chem. Rev.*, 2008, **108**, 74–108.
8 M. Ahmed, M. Blum, E. J. Crumlin, P. L. Geissler, T. Head-Gordon, D. T. Limmer, K. K. Mandadapu, R. J. Saykally and K. R. Wilson, Molecular Properties and Chemical Transformations Near Interfaces, *J. Phys. Chem. B*, 2021, **125**(32), 9037–9051.
9 M. Bonn, Concluding remarks for Faraday Discussion on Water at Interfaces, *Faraday Discuss.*, 2024, **249**, 521–525.
10 N. Agmon, H. J. Bakker, R. K. Campen, R. H. Henchman, P. Pohl, S. Roke, M. Thämer and A. Hassanali, Protons and Hydroxide Ions in Aqueous Systems, *Chem. Rev.*, 2016, **116**, 7642–7672.
11 D. L. McCaffrey, S. C. Nguyen, S. J. Cox, H. Weller, A. P. Alivisatos, P. L. Geissler and R. J. Saykally, Mechanism of ion adsorption to aqueous interfaces: Graphene/water vs. air/water, *Proc. Natl. Acad. Sci.*, 2017, **114**(51), 13369–13373.
12 S. Pullanchery, S. Kulik, B. Rehl, A. Hassanali and S. Roke, Charge transfer across C–H···O hydrogen bonds stabilizes oil droplets in water, *Science*, 2021, **374**, 1366–1370.
13 E. Poli, K. H. Jong and A. Hassanali, Charge transfer as a ubiquitous mechanism in determining the negative charge at hydrophobic interfaces, *Nat. Commun.*, 2020, **11**, 901.
14 J. Nauruzbayeva, Z. Sun, A. Gallo, M. Ibrahim, J. C. Santamarina and H. Mishra, Electrification at water–hydrophobe interfaces, *Nat. Commun.*, 2020, **11**, 5285.
15 S. W. Devlin, F. Bernal, E. J. Riffe, K. R. Wilson and R. J. Saykally, Spiers Memorial Lecture: Water at interfaces, *Faraday Discuss.*, 2024, **249**, 9–37.
16 I. Nam, H. G. Nam and R. N. Zare, Abiotic synthesis of purine and pyrimidine ribonucleosides in aqueous microdroplets, *Proc. Natl. Acad. Sci.*, 2018, **115**, 36.
17 S. Banerjee, E. Gnanamani, X. Yan and R. N. Zare, Can all bulk-phase reactions be accelerated in microdroplets?, *Analyst*, 2017, **142**, 1399–1402.
18 K.-H. Huang, N. M. Morato, Y. Feng and R. G. Cooks, High-throughput Diversification of Complex Bioactive Molecules by Accelerated Synthesis in Microdroplets, *Angew. Chem., Int. Ed.*, 2023, e202300956.
19 D. T. Holden, N. M. Morato and R. G. Cooks, Aqueous microdroplets enable abiotic synthesis and chain extension of unique peptide isomers from free amino acids, *Proc. Natl. Acad. Sci.*, 2022, **119**, e2212642119.
20 G. Rovelli, M. I. Jacobs, M. D. Willis, R. J. Rapf, A. M. Prophet and K. R. Wilson, A critical analysis of electrospray techniques for the determination of accelerated rates and mechanisms of chemical reactions in droplets, *Chem. Sci.*, 2020, **11**, 13026–13043.
21 D. Nguyen, S. Casillas, H. Vang, A. Garcia, H. Mizuno, E. J. Riffe, R. J. Saykally and S. C. Nguyen, Catalytic Mechanism of Interfacial Water in the Cycloaddition of Quadricyclane and Diethyl Azodicarboxylate, *J. Phys. Chem. Lett.*, 2021, **12**, 3026–3030.
22 E. C. Griffith and V. Vaida, In situ observation of peptide bond formation at the water–air interface, *Proc. Natl. Acad. Sci.*, 2012, **109**, 15697–15701.
23 Z. Wei, Y. Li, R. G. Cooks and X. Yan, Accelerated Reaction Kinetics in Microdroplets: Overview and Recent Developments, *Annu. Rev. Phys. Chem.*, 2020, **71**, 31–51.
24 L. Qiu and R. G. Cooks, Spontaneous Oxidation in Aqueous Microdroplets: Water Radical Cation as Primary Oxidizing Agent, *Angew. Chem., Int. Ed.*, 2024, e202400118.
25 M. F. Ruiz-Lopez, Midair transformations of aerosols, *Science*, 2021, **374**, 686–687.
26 J. M. Schiffer, L. E. Mael, K. A. Prather, R. E. Amaro and V. H. Grassian, Sea Spray Aerosol: Where Marine Biology Meets Atmospheric Chemistry, *ACS Cent. Sci.*, 2018, **4**, 1617–1623.
27 M. Mofidfar, M. A. Mehrgardi, Y. Xia and R. N. Zare, Dependence on relative humidity in the formation of reactive oxygen species in water droplets, *Proc. Natl. Acad. Sci.*, 2024, **121**, e2315940121.
28 V. Stadnytskyi, P. Anfinrud and A. Bax, Breathing, speaking, coughing or sneezing: What drives transmission of SARS-CoV-2?, *J. Intern. Med.*, 2021, **290**, 1010–1027.
29 V. Vaida, Prebiotic phosphorylation enabled by microdroplets, *Proc. Natl. Acad. Sci.*, 2017, **114**, 12359–12361.
30 J. H. Seinfeld and S. N. Pandis, *Atmospheric Chemistry and Physics: From Air Pollution to Climate Change*, Wiley-Interscience, 2nd edn, 2006, 1998.
31 H. R. Pruppacher and J. D. Klett, *Microphysics of Clouds and Precipitation*, D. Reidel Publishing Company, Holland, 1980.
32 H. Mishra, R. J. Nielsen, S. Enami, M. R. Hoffmann, A. J. Colussi and W. A. Goddard, Quantum chemical insights into the dissociation of nitric acid on the surface of aqueous electrolytes, *Int. J. Quantum Chem.*, 2013, **113**, 413–417.
33 D. Hillel, *Introduction to Soil Physics*, Academic Press, 1982.
34 J. A. Otter, S. Yezli, F. Barbut and T. M. Perl, An overview of automated room disinfection systems: When to use them and how to choose them, *Decontamination in Hospitals and Healthcare*, 2020, pp. 323–369.
35 S. Pillai, A. Santana, R. Das, B. R. Shrestha, E. Manalastas and H. Mishra, A molecular to macro level assessment of direct contact membrane distillation for separating organics from water, *J. Membr. Sci.*, 2020, **608**, 118140.
36 M. M. Benjamin, *Water Chemistry*, Waveland Press, Inc., Long Grove, IL, USA, 2nd edn, 2015.
37 F. Garcia-Ochoa and E. Gomez, Bioreactor scale-up and oxygen transfer rate in microbial processes: an overview, *Biotechnol. Adv.*, 2009, **27**, 153–176.
38 M. Ali, P.-Y. Hong, H. Mishra, J. Vrouwenvelder and P. E. Saikaly, Adopting the circular model: opportunities and challenges of transforming wastewater treatment

Open Access Article. Published on 18 November 2024. Downloaded on 2/16/2026 4:10:19 PM. This article is licensed under a Creative Commons Attribution-NonCommercial 3.0 Unported Licence.

plants into resource recovery factories in Saudi Arabia, *Water Reuse*, 2022, **12**, 346–365.
39 A. Santana, A. S. F. Farinha, A. Z. Torano, M. Ibrahim and H. Mishra, A first-principles approach for treating wastewaters, *Int. J. Quantum Chem.*, 2021, **121**(5), e26501.
40 A. J. Bard and L. R. Faulkner, *Electrochemical Methods: Fundamentals and Applications*, John Wiley & Sons, 2nd edn, 2001.
41 H. Mishra, B. A. Cola, V. Rawat, P. B. Amama, K. G. Biswas, X. F. Xu, T. S. Fisher and T. D. Sands, Thermomechanical and Thermal Contact Characteristics of Bismuth Telluride Films Electrodeposited on Carbon Nanotube Arrays, *Adv. Mater.*, 2009, **21**(42), 4280–4283.
42 E. De Hoffmann and V. Stroobant, *Mass spectrometry: principles and applications*, John Wiley & Sons, 2007.
43 A. J. Ingram, C. L. Boeser and R. N. Zare, Going beyond electrospray: mass spectrometric studies of chemical reactions in and on liquids, *Chem. Sci.*, 2016, **7**, 39–55.
44 S. Enami, H. Mishra, M. R. Hoffmann and A. J. Colussi, Protonation and Oligomerization of Gaseous Isoprene on Mildly Acidic Surfaces: Implications for Atmospheric Chemistry, *J. Phys. Chem. A*, 2012, **116**, 6027–6032.
45 A. J. Colussi, S. Enami and S. Ishizuka, Hydronium Ion Acidity Above and Below the Interface of Aqueous Microdroplets, *ACS Earth Space Chem.*, 2021, **5**, 2341–2346.
46 A. Gallo, A. S. F. Farinha, M. Dinis, A.-H. Emwas, A. Santana, R. J. Nielsen, W. A. Goddard and H. Mishra, The chemical reactions in electrosprays of water do not always correspond to those at the pristine air–water interface, *Chem. Sci.*, 2019, **10**, 2566–2577.
47 A. J. Colussi and S. Enami, Comment on "The chemical reactions in electrosprays of water do not always correspond to those at the pristine air–water interface" by A. Gallo Jr, A. S. F. Farinha, M. Dinis, A.-H. Emwas, A. Santana, R. J. Nielsen, W. A. Goddard III and H. Mishra, *Chem. Sci.*, 2019, **10**(2566), 8253–8255.
48 A. Gallo, A. S. F. Farinha, A.-H. Emwas, A. Santana, R. J. Nielsen, W. A. Goddard and H. Mishra, Reply to the 'Comment on "The chemical reactions in electrosprays of water do not always correspond to those at the pristine air–water interface"' by A. J. Colussi and S. Enami, Chem. Sci., 2019, 10, DOI: 10.1039/c9sc00991d, *Chem. Sci.*, 2019, **10**(1039), 8256–8261.
49 M. I. Jacobs, R. D. Davis, R. J. Rapf and K. R. Wilson, Studying Chemistry in Micro-compartments by Separating Droplet Generation from Ionization, *J. Am. Soc. Mass Spectrom.*, 2019, **30**, 339–343.
50 M. T. Martins-Costa and M. F. Ruiz-López, Probing solvation electrostatics at the air–water interface, *Theor. Chem. Acc.*, 2023, **142**, 29.
51 K. R. Wilson and A. M. Prophet, Chemical Kinetics in Microdroplets, *Annu. Rev. Phys. Chem.*, 2024, **75**, 185–208.
52 J. K. Lee, K. L. Walker, H. S. Han, J. Kang, F. B. Prinz, R. M. Waymouth, H. G. Nam and R. N. Zare, Spontaneous generation of hydrogen peroxide from aqueous microdroplets, *Proc. Natl. Acad. Sci. U. S. A.*, 2019, **116**, 19294–19298.
53 M. T. Dulay, C. A. Huerta-Aguilar, C. F. Chamberlayne, R. N. Zare, A. Davidse and S. Vukovic, Effect of relative humidity on hydrogen peroxide production in water droplets, *QRB Discovery*, 2021, **2**, e8.
54 J. K. Lee, H. S. Han, S. Chaikasetsin, D. P. Marron, R. M. Waymouth, F. B. Prinz and R. N. Zare, Condensing water vapor to droplets generates hydrogen peroxide, *Proc. Natl. Acad. Sci. U. S. A.*, 2020, **117**, 30934–30941.
55 M. A. Mehrgardi, M. Mofidfar and R. N. Zare, Sprayed Water Microdroplets Are Able to Generate Hydrogen Peroxide Spontaneously, *J. Am. Chem. Soc.*, 2022, **144**, 7606–7609.
56 J. P. Heindel, H. Hao, R. A. LaCour and T. Head-Gordon, Spontaneous formation of hydrogen peroxide in water microdroplets, *J. Phys. Chem. Lett.*, 2022, **13**, 10035–10041.
57 H. Hao, I. Leven and T. Head-Gordon, Can electric fields drive chemistry for an aqueous microdroplet?, *Nat. Commun.*, 2022, **13**, 280.
58 J. P. Heindel, R. A. LaCour and T. Head-Gordon, The role of charge in microdroplet redox chemistry, *Nat. Commun.*, 2024, **15**, 3670.
59 K. Gong, A. Nandy, Z. Song, Q.-S. Li, A. Hassanali, G. Cassone, S. Banerjee and J. Xie, Revisiting the Enhanced Chemical Reactivity in Water Microdroplets: The Case of a Diels–Alder Reaction, *J. Am. Chem. Soc.*, 2024, **146**(46), 31585–31596.
60 A. J. Colussi, Mechanism of Hydrogen Peroxide Formation on Sprayed Water Microdroplets, *J. Am. Chem. Soc.*, 2023, **145**, 16315–16317.
61 A. Gallo Jr, N. H. Musskopf, X. Liu, Z. Yang, J. Petry, P. Zhang, S. Thoroddsen, H. Im and H. Mishra, On the formation of hydrogen peroxide in water microdroplets, *Chem. Sci.*, 2022, **13**, 2574–2583.
62 N. H. Musskopf, A. Gallo, P. Zhang, J. Petry and H. Mishra, The Air–Water Interface of Water Microdroplets Formed by Ultrasonication or Condensation Does Not Produce H2O2, *J. Phys. Chem. Lett.*, 2021, **12**, 11422–11429.
63 M. A. Eatoo and H. Mishra, Busting the myth of spontaneous formation of H2O2 at the air–water interface: contributions of the liquid–solid interface and dissolved oxygen exposed, *Chem. Sci.*, 2024, **15**, 3093–3103.
64 R. Trager, Water microdroplet chemistry is contentious, here's why, **https://www.chemistryworld.com/news/water-microdroplet-chemistry-is-contentious-heres-why/4018721.article.Journal**, 2024.
65 J. K. Lee, D. Samanta, H. G. Nam and R. N. Zare, Spontaneous formation of gold nanostructures in aqueous microdroplets, *Nat. Commun.*, 2018, **9**, 1562.
66 C. Gutiérrez-Wing, R. Esparza, C. Vargas-Hernández, M. E. Fernández García and M. José-Yacamán, Microwave-assisted synthesis of gold nanoparticles self-assembled into self-supported superstructures, *Nanoscale*, 2012, **4**, 2281–2287.
67 T. Kakeshpour and A. Bax, NMR characterization of H2O2 hydrogen exchange, *J. Magn. Reson.*, 2021, **333**, 107092.
68 W. H. Koppenol, D. M. Stanbury and P. L. Bounds, Electrode potentials of partially reduced oxygen species, from dioxygen to water, *Free Radical Biol. Med.*, 2010, **49**, 317–322.

© 2025 The Author(s). Published by the Royal Society of Chemistry

Open Access Article. Published on 18 November 2024. Downloaded on 2/16/2026 4:10:19 PM.
This article is licensed under a Creative Commons Attribution-NonCommercial 3.0 Unported Licence.

69 A. V. Naumkin, A. Kraut-Vass, S. W. Gaarenstroom, and C. J. Powell, *X-ray Photoelectron Spectroscopy Database*, National Institute of Standards and Technology, 2022, DOI: 10.18434/T4T88K.
70 C. J. Chen and E. Williams, Are Hydroxyl Radicals Spontaneously Generated in Unactivated Water Droplets?, *Angew. Chem., Int. Ed.*, 2024, e202407433.
71 D. Nguyen, P. Lyu and S. C. Nguyen, Experimental and Thermodynamic Viewpoints on Claims of a Spontaneous H2O2 Formation at the Air–Water Interface, *J. Phys. Chem. B*, 2023, **127**, 2323–2330.
72 D. Nguyen and S. C. Nguyen, Revisiting the Effect of the Air–Water Interface of Ultrasonically Atomized Water Microdroplets on H2O2 Formation, *J. Phys. Chem. B*, 2022, **126**, 3180–3185.
73 D. Nguyen and S. C. Nguyen, Revisiting the Effect of the Air–Water Interface of Ultrasonically Atomized Water Microdroplets on H2O2 Formation, *J. Phys. Chem. B*, 2022, **126**, 3180–3185.
74 W. H. Koppenol and H. Sies, Was hydrogen peroxide present before the arrival of oxygenic photosynthesis? The important role of iron(II) in the Archean ocean, *Redox Biol.*, 2024, **69**, 103012.
75 M. Angelaki, Y. Carreira Mendes Da Silva, S. Perrier and C. George, Quantification and Mechanistic Investigation of the Spontaneous H2O2 Generation at the Interfaces of Salt-Containing Aqueous Droplets, *J. Am. Chem. Soc.*, 2024, **146**, 8327–8334.
76 L. E. Krushinski and J. E. Dick, Direct electrochemical evidence suggests that aqueous microdroplets spontaneously produce hydrogen peroxide, *Proc. Natl. Acad. Sci.*, 2024, **121**, e2321064121.
77 K. Li, Y. Guo, S. A. Nizkorodov, Y. Rudich, M. Angelaki, X. Wang, T. An, S. Perrier and C. George, Spontaneous dark formation of OH radicals at the interface of aqueous atmospheric droplets, *Proc. Natl. Acad. Sci.*, 2023, **120**, e2220228120.
78 M. Angelaki, J. d'Erceville, D. J. Donaldson and C. George, pH Affects the Spontaneous Formation of H2O2 at the Air–Water Interfaces, *J. Am. Chem. Soc.*, 2024, **146**, 25889–25893.
79 N. T. K. Thanh, N. Maclean and S. Mahiddine, Mechanisms of Nucleation and Growth of Nanoparticles in Solution, *Chem. Rev.*, 2014, **114**, 7610–7630.
80 D. R. Baer, Guide to making XPS measurements on nanoparticles, *J. Vac. Sci. Technol. A*, 2020, **38**, 031201.

© 2025 The Author(s). Published by the Royal Society of Chemistry